Arabian Journal of Chemistry (2019) 12, 1134–1140

King Saud University

Arabian Journal of Chemistry

www.ksu.edu.sa
www.sciencedirect.com

ORIGINAL ARTICLE

Silver embedded C-TiO_2 exhibits improved photocatalytic properties with potential application in waste water treatment

Mohamed Elfatih Hassan [b,*], Guanglong Liu [a,*], Eltigani Osman Musa Omer [b], Arafat M. Goja [c], Sadananda Acharya [b]

[a] *Laboratory of Plant Nutrition and Ecological Environment Research, Centre for Microelement Research of Huazhong Agricultural University, Wuhan 430070, China*
[b] *Department of Public Health, College of Public Health, Imam Abdulrahman Bin Faisal University, Dammam, P.O. Box 1982, Dammam, Saudi Arabia*
[c] *Department of Clinical Nutrition, College of Applied Medical Sciences, Imam Abdulrahman Bin Faisal University, Dammam, P.O. Box 1982, Dammam, Saudi Arabia*

Received 22 September 2018; accepted 11 December 2018
Available online 17 December 2018

KEYWORDS

C-TiO_2/Ag;
Photocatalytic properties;
Organic pollutant;
Water treatment

Abstract Non-metal element doping on photocatalysts demonstrates a wide range of disadvantages. Hence metal embedding on nanomaterials is considered to enhance photocatalytic efficiency. In this study, we employed silver nano particle embedding on C-TiO_2 photocatalyst to improve its phtotocatytic degradation efficiency of organic water pollutant such as methyl orange. Modified sol-gel methods based on self-assembly technique was used to prepare the nanoformulations. The synthesized nanoparticles were characterized by X-Ray diffraction (XRD), Fourier transforms infrared (FT-IR), Scanning electron microscopy (SEM), X-ray photoelectron spectroscopy (XPS), UV–vis diffuse reflectance spectroscopy, and photoluminescence spectra (PL). Compared to non-silver formulation (C-TiO_2), silver embedded nanomaterial (C-TiO_2/Ag) displayed an increased shift in the light absorption towards visible spectrum. A low photoluminescence (PL) intensity by 1 wt% C-TiO_2/Ag indicated improved photocatalytic efficiency. Further, higher degradation of organic dye methyl orange confirmed that 1 wt% C-TiO_2/Ag exhibited the best photodegradation rate over its non Ag embedded C-TiO_2. Embedding of silver on C-TiO_2 extends optical absorption edge of C-TiO_2 to more visible spectrum and inhibits electron-hole recombination resulting in enhanced photocatalytic activity. Photocatalytic degradation on methyl orange

* Corresponding authors at: Department of Public Health, College of Public Health, Imam Abdulrahman Bin Faisal University, Dammam, P.O. Box 1982, Dammam, Saudi Arabia (M.E. Hassan).
E-mail addresses: mehahmed@iau.edu.sa (M.E. Hassan), liugl@mail.hzau.edu.cn (G. Liu).

Peer review under responsibility of King Saud University.

ELSEVIER Production and hosting by Elsevier

https://doi.org/10.1016/j.arabjc.2018.12.004

organic pollutant was considerably improved indicating its potential use in water treatment applications.

1. Introduction

Degradation of environmental organic pollutants and toxic materials by semiconductor photocatalysis, one of the advanced physicochemical processes, has been largely used in waste water treatment (Ollis and Al-Ekabi, 1993; Xu et al., 2011). Most of the studies in this field focused on titanium dioxide (TiO_2) owing to its advantages compared to other oxide semiconductor photocatalysts. TiO_2 is nontoxic, highly stable, strong oxidizer and possesses excellent biological and chemical properties. Additionally, its capacity to completely mineralize pollutants, resistance to photo-corrosion, proven environmental safety, availability and cost-effectiveness have made TiO_2 a popular nanomaterial in multiple applications (Kosowska et al., 2005; Duan et al., 2012). However, TiO_2 has some drawbacks; for instance, it primarily absorbs UV light under wavelength less than 380 nm, which is only 5% of the solar light. Moreover, with rapid recombination of photogenerated electrons and holes; the quantum yield of TiO_2 photocatalysis is usually very low (Emeline et al., 2006; Fang et al., 2008). Therefore, these pitfalls limit the application of TiO_2 for environmental remediation with solar light and O_2. Recently, many researchers have focused on this area to improve the efficiency of TiO_2 photocatalysis, and to develop a visible light photocatalyst. One of the common strategies to achieve this is "*doping*" TiO_2 with non-metals. Carbon has been suggested to improve the photocatalysis of TiO_2 because of its narrow band gap (Lettmann et al., 2001; Khan et al., 2002; Sakthivel and Kisch, 2003; Barborini et al., 2005; Gu et al., 2008; Mai et al., 2009). Incorporation of non-metal improves light absorption, but in contrast assists in increasing the recombination rate of electron and hole and consequently leads to an overall reduction in performance (Xu et al., 2011).

Lately, some studies have been carried out to improve the photocatalytic efficiency of TiO_2 using precious metals such as gold (Au), silver (Ag), and platinum (Pt) which can inhibit the recombination of charge carriers (Tom et al., 2003; Hirakawa and Kamat, 2005; Matsubara and Tatsuma, 2007; Kumar and Devi, 2011). Principally, most of these studies focused on degradation of organic dyes and organic pesticides using photo-oxidation method (Kumar and Devi, 2011; Maicu et al., 2011). Generally, metallic nanoparticles can be used with different methods; for example, fixed in frameworks or added on surfaces, to work as electron catchers, metallic receptors or interfacial charge transfer factors. Novel characteristics of the metallized TiO_2 have been debated in photocatalytic applications such as surface plasmon resonance states, visible-light-driven photoactivity, recombination rate of photogenerated electrons and holes. Nevertheless this subject is understudied because of the properties of the metallic nanoparticles that affect the TiO_2 framework (Choi et al., 2009; Kumar and Devi, 2011).

In the present work, we aimed to develop a silver embeded C-TiO_2 [C-TiO_2/Ag] nanomaterial and evaluate its possibly improved photocatalytic properties on an experimental methyl orange (MeO) organic pollutant containing water sample.

2. Material and methods

2.1. Materials

Tween 80 [T80, polyoxyethylenesorbitanmonooleate], Isopropanol 99.8% ((CH3)2CHOH), acetic acid (CH_3COOH), all from Guoyao Chemical Reagent Co. Ltd, Shanghai, China; Nitric acid (HNO_3) [0.05 mol L^{-1}], Silver nitrate ($AgNO_3$), Methyl orange ($C_{14}H_{14}N_3NaO_3S$) all from Sinopharm Chemical Reagent Co. Ltd, Shanghai, China and titanium tetraisopropoxide (TTIP, 97%) from Sigma-Aldrich, St. Louis, Missouri, USA were procured commercially and used in the experiments.

2.2. Synthesis of C-TiO_2

C-TiO_2 nanoparticle photocatalysts were synthesized by using a sol–gel technique. Tween 80 (T80) was used as the carbon precursor and fixed in the modified sol-gel solution. T80 (5 ml) was mixed with 20 ml of isopropanol, and then 3 ml titanium tetraisopropoxide was added and was dissolved under continuous stirring condition for 24 h. Then, 3 ml of acetic acid was added into the total volume of solutions in order to achieve consistency of the admixture. The solution was kept for one day at room temperature and stirring condition to obtain a homogeneous and steady solution. Then the solution was incubated at 60 °C for 3 h, to get the sol–gel. Finally, the sol–gel was calcined in an advanced furnace under 400 °C for 3 h, and cooled down naturally and the C-TiO_2 nanoparticles thus obtained were collected.

2.3. Preparation of C-TiO_2/Ag

To prepare C-TiO_2/Ag nanoparticles, a slurry was prepared by mixing of C-TiO_2 powder with 50 ml of $AgNO_3$ alcoholic solution. The mixture was maintained under continuous stirring condition for 30 mins to obtain an adsorption equilibrium of the silver ions on the C-TiO_2 surface. Thereafter, the slurry was irradiated at room temperature using a commercial germicidal lamp (TecnoLite G15T8, Mexico, 214 nm, 17 W) for 60 min under vigorous stirring. The obtained solution was dried overnight in an hot air oven at 100 °C. The silver nanocomposites as (0.5, 1, 2, and 5 wt% Ag)/C-TiO_2 and 1%Ag/TiO_2 were prepared.

2.4. Characterization of C-TiO_2/Ag

X-ray diffraction (XRD) pattern of the synthesized nanomaterial was analysed in Rigaku Multiplex system, Rigaku Corporation, Tokyo, Japan) with the Cu Kα (λ = 1.5406 Å)

radiation to ascertain crystallinity and phase of the samples. An X-ray photoelectron spectroscope (XPS, PerkinElmer Model 5300; Perkin Elmer, Waltham, Massachusetts, USA) was employed to determine fine elemental composition and electronic structure. Field-emission scanning electron microscope (FE-SEM) analysis was performed on a Hitachi S-4800 (Hitachi Hi-Technologies Corp., Tokyo, Japan). Fourier transform infrared (FT-IR) spectroscopy (FTIR Spectrometer Alpha II; Brucker, Massachusetts, USA) was conducted to detect chemical groups in the prepared catalysts. UV–vis absorption spectra of the nanomaterial was acquired using a UV–vis spectrophotometer (Shimadzu 2450 PC; Shimadzu Corporation, Kyoto, Japan), which was installed with an incorporating sphere supplement (ISR1200) using $BaSO_4$ as standard to examine the light absorption of the prepared nanoparticle catalysts (with the range of wavelength 240–800 nm). Photoluminescence spectra (PL) of the material was assessed at 25 °C on a Shimadzu RF-5301 PC spectrometer (Shimadzu Corporation, Kyoto, Japan) using excitation light EX = 240 nm and emission spectrometry range EM = 350–400 nm.

2.5. Photocatalytic degradation experiment

Photocatalytic performance of the synthesized nanomaterials was studied by degradation of Methyl orange, one of the organic water pollutants in water under visible light irradiation. First, a particle suspension of the catalyst (0.5 g) was dissolved in one liter of aqueous solution using a stirrer kept stirring for onvernight. Then, 400 µL of methyl orange solution (250 mg/L) was placed on 50 ml particle suspension. Finally, to ensure the acidity of the degradation system 50 µL of Nitric acid was added to the solution. The solution was placed under xenon light source, (xenon lamp current value was adjusted at 15 A, with UV filters to remove UV light to ensure all the light is within visible spectrum). To study its effect on photodegradation, 50 µL of hydrogen peroxide (H_2O_2) was added into the solution. A 5 ml sample was withdrawn at time 0, 30, 60, 90, 120, 150, and 180 min. The photocatalyst was promptly isolated from the sample specimens after centrifugation (5000) rpm for 10 min in room temperature. The development of photocatalytic breakdown was observed by the measurement of characteristic absorbance of the solution samples using a UV–vis spectrophotometer (Shimadzu 2450 PC; Shimadzu Corporation, Kyoto, Japan).

3. Results and discussion

3.1. XRD reveals anatase TiO_2 phase and increased crystalline size of C-TiO_2/Ag

XRD were used to study crystal structure and crystal phase characterizations of the synthesized C-TiO_2/Ag. Since the photocatalytic efficiency of catalyst was highly affected by its crystallinity and the phase of the catalyst (Pelaez et al., 2009), TiO_2 anatase phase was reported with high photocatalytic activity compared with other crystalline forms (Ollis and Al-Ekabi, 1993; Kosowska et al., 2005). The XRD patterns of synthesised TiO_2, C-TiO_2, Ag-TiO_2 and C-TiO_2/Ag are shown in Fig. 1. The distinct diffraction peaks at 2θ of 25.3°, 37.8°,48°, 53.9°, 62.7°, 70.3° and 75° corresponding to (1 0 1), (0 0 4), (2 0 0), (1 0 5), (2 0 4), (2 2 0) and (2 1 5) crystal faces of anatase TiO_2 were identified in all the samples which indicated that the presence of anatase TiO_2 phase in all the samples. Similar to our results, Huang et al. (2018) also reported that Ag nanoparticles uniformly embedded in the anatase TiO_2 nanotubes walls and brought large interfacial area between Ag particles and TiO_2 nanotubes indicating transformation of Ag-TiO_2 into anatase TiO_2. It can be observed that a major peak at 25.3° in C-TiO_2/Ag became narrow, which attributed to the increase in the crystallite size of titanium dioxide (TiO_2), whereas XRD pattern of C-TiO_2 does not displays any peak corresponding to silver crystal phases.

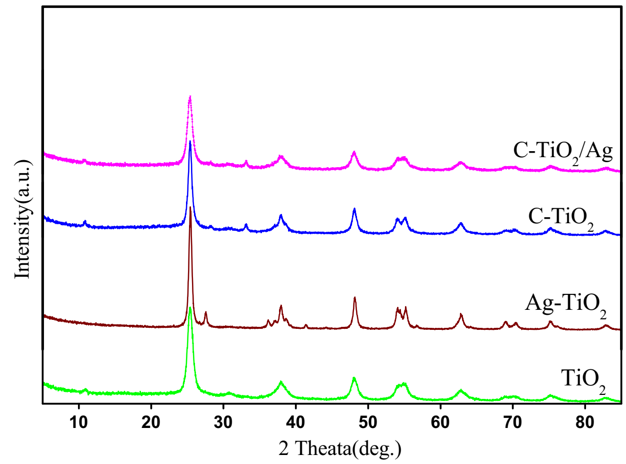

Fig. 1 XRD patterns of C-TiO_2 (reference) and Ag/C-TiO_2.

3.2. Scaning electron microscopy (SEM) shows improved specific surface area of C-TiO_2/Ag

It is visible that C-TiO_2/Ag nanoparticles are mainly presented as cube-like shape in scanning electron microscopy (SEM) as shown in Fig. 2(a & b). However, the surface Ag nanoparticles are unable to present the same feature (Fig. 2b); which may be due to less contents and small particle size of silver. It can be seen from Fig. 2a and b that the samples of C-TiO_2 and C-TiO_2/Ag showed fairly rough surface, on the other hand, little shining silver grains and very small punctures are observed on the surface of C-TiO_2/Ag (Fig. 2b). This indicates an improved specific surface area of the nanoparticles C-TiO_2 achieved by Ag embedding as evidenced in earlier studies where Ag compounds were used to embed TiO_2 (Huang et al., 2018). Higher specific surface area of photocatalyst could provide increased contact area with the organic pollutant such as methyl orange during photocatalytic reaction and may improve its activity. Transmission Electron Microscopy (TEM) analysis of Ag embedded TiO_2 had earlier revealed that the techinique is helpful in maintaining the tubular structure of nanomaterial because of the uniform distribution of Ag ions on the nanomaterial (Huang et al., 2018). Similar results were also noticed by Naraginti et al. (2015).

3.3. FT-IR spectroscopy indicates intense strength of O-H bonded group in C-TiO_2/Ag

The infrared spectra of TiO_2, Ag-TiO_2, C-TiO_2 and C-TiO_2/Ag samples are shown in Fig. 3. The bands at 1640 and 3380 cm^{-1}

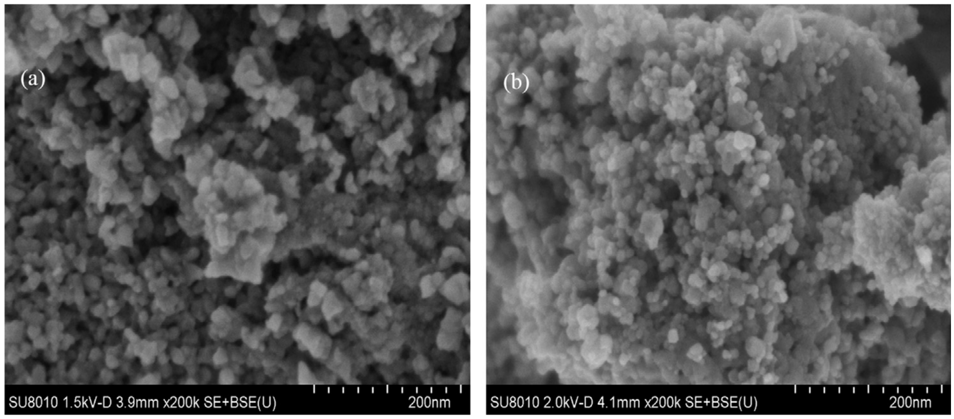

Fig. 2 The SEM images of the (a) C-TiO$_2$ and (b) Ag/C-TiO$_2$.

are nascent from O—H stretching of adsorbed H_2O molecules. Many reports confirmed that O—H group on the catalyst surface may consider as a very important factor in enhancing photocatalysis efficiency of TiO$_2$ and inhibiting the recombination rate of charge carriers. From Fig. 3 it can be noticed that the strength of hydroxyl bonded group in C-TiO$_2$/Ag sample was more intense than that of other samples. From the result, the bands at 2330 cm^{-1} are due to the stretching vibrations of C═O, indicating the residual C element in all the catalyst surface except the Ag-TiO$_2$, which might have come from Tween 80 used in the sol preparation. The same band also appeared in TiO$_2$ sample; which may be due to absorption of CO_2 from air during the preparation process (Kumar and Devi, 2011). Meanwhile, the peaks around 1380 cm^{-1} in Ag-TiO$_2$ and C-TiO$_2$/Ag are due to NO_3^- bonds, which attributed to the $AgNO_3$ used in the preparation samples.

3.4. The UV–vis absorption spectra of C-TiO$_2$/Ag exhibits increased light absorption

UV–vis spectroscopy of 1% C-TiO$_2$/Ag and the C-TiO$_2$ (reference) are presented in Fig. 4. From the results, it is interesting to notice that C-TiO$_2$ embedded with silver (C-TiO$_2$/Ag) could significantly exhibit red shift to higher wave length. This result can be referred to the arrangement of Ag nanoparticles on the surface of TiO$_2$, which influenced insulation constant of the surrounding matrix and eventually promoting the visible light absorption of C-TiO$_2$ (Ung et al., 1998). Earlier studies wherein TiO$_2$ was embedded with Ag compounds also showed enhanced response in visible region of the light (Huang et al., 2018). While doping TiO$_2$ with Ag, Naraginti et al. (2015) calculated energy gap value of the composite to be 2.87 eV, indicating decrease in band energy and increase in wavelength value due to red shft. The authors also opined that this shift in the optical property of the composite had resulted in better photocatalytic abilities of the Ag embedded TiO$_2$.

3.5. Photoluminescence spectra (PL) of C-TiO$_2$/Ag shows lower electron-hole recombination rate thus improving its photocatalytic efficiency

Photoluminescence (PL) emission spectra is produced from recombination of electron and hole (Li et al., 2005). PL results could be helpful in studying the efficiency of charge carrier

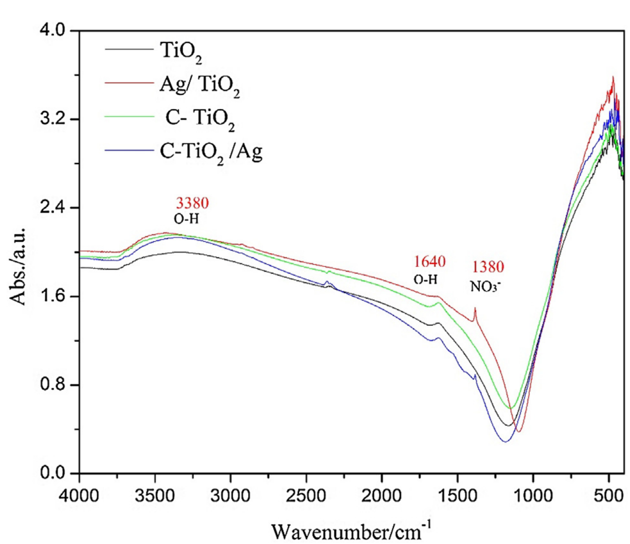

Fig. 3 FT-IR spectra of TiO$_2$, Ag/TiO$_2$, C-TiO$_2$ and Ag/C-TiO$_2$.

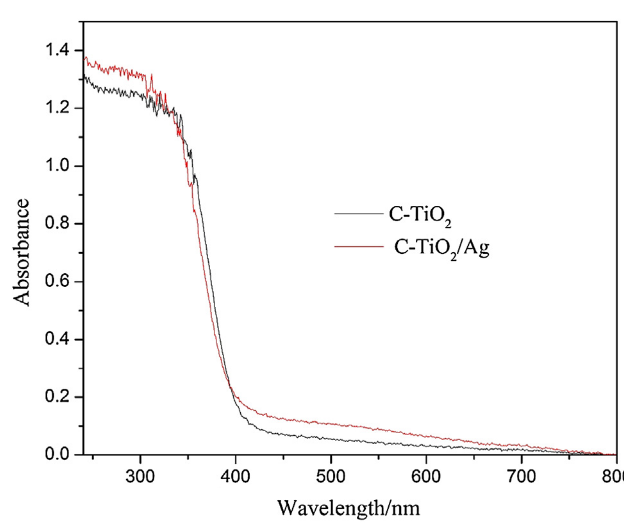

Fig. 4 The UV–vis absorption spectra of C-TiO$_2$ and Ag/C-TiO$_2$ samples.

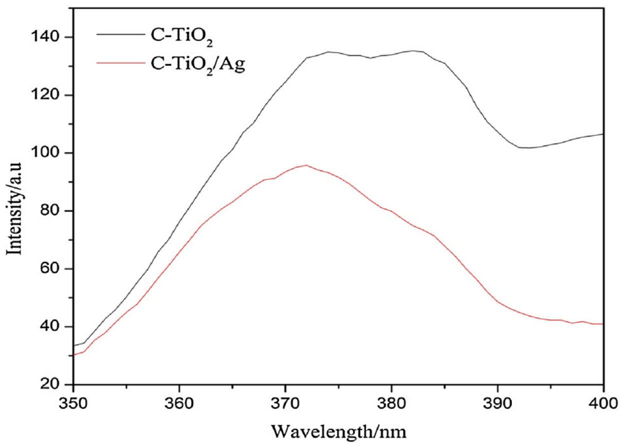

Fig. 5 Photoluminescence spectra of Ag/C-TiO_2 and C-TiO_2 (Reference).

trapping, its movement, and also to know the intensity of photo-generated electrons and holes and its fate. It is well known that the recombination rate of photogenerated electrons and holes is very important factor affecting the photocatalytic performance. Fig. 5 shows the PL spectra of C-TiO_2 and C-TiO_2/Ag nanoparticles. The emission intensity peaks of C-TiO_2/Ag and C-TiO_2 catalyst at 372 nm were about 85.95 and 130.39 arbitrary unit (au), respectively. When TiO_2-C-Ag composites are irradiated by visible light, shift in electron from valence band to conduction band creates a hole in valence band (Naraginti et al., 2015). Recombination of these holes reduces the photocatalytic activity of the composite material. Ag embedded in C-TiO_2 could trap the electron inhibiting hole recombination thus increasing the photocatalytic activity (Pantelides, 1978; Subash et al., 2012). In the present study, emission peak of C-TiO_2/Ag is lower than that of C-TiO_2, indicating that the addition of Ag improves the efficiency of C-TiO_2 and reduced the electron-hole recombination rate. This result can be attributed to the phenomenon that the electrons are excited from valence band to conduction band and then relocated to silver, due to the outstanding electronic conductivity of silver and prevented the recombination of electrons and holes. Huang et al. (2018) reported that Ag embedding of TiO_2 enhanced the separation effect of photogenerated electron hole pair in TiO_2.

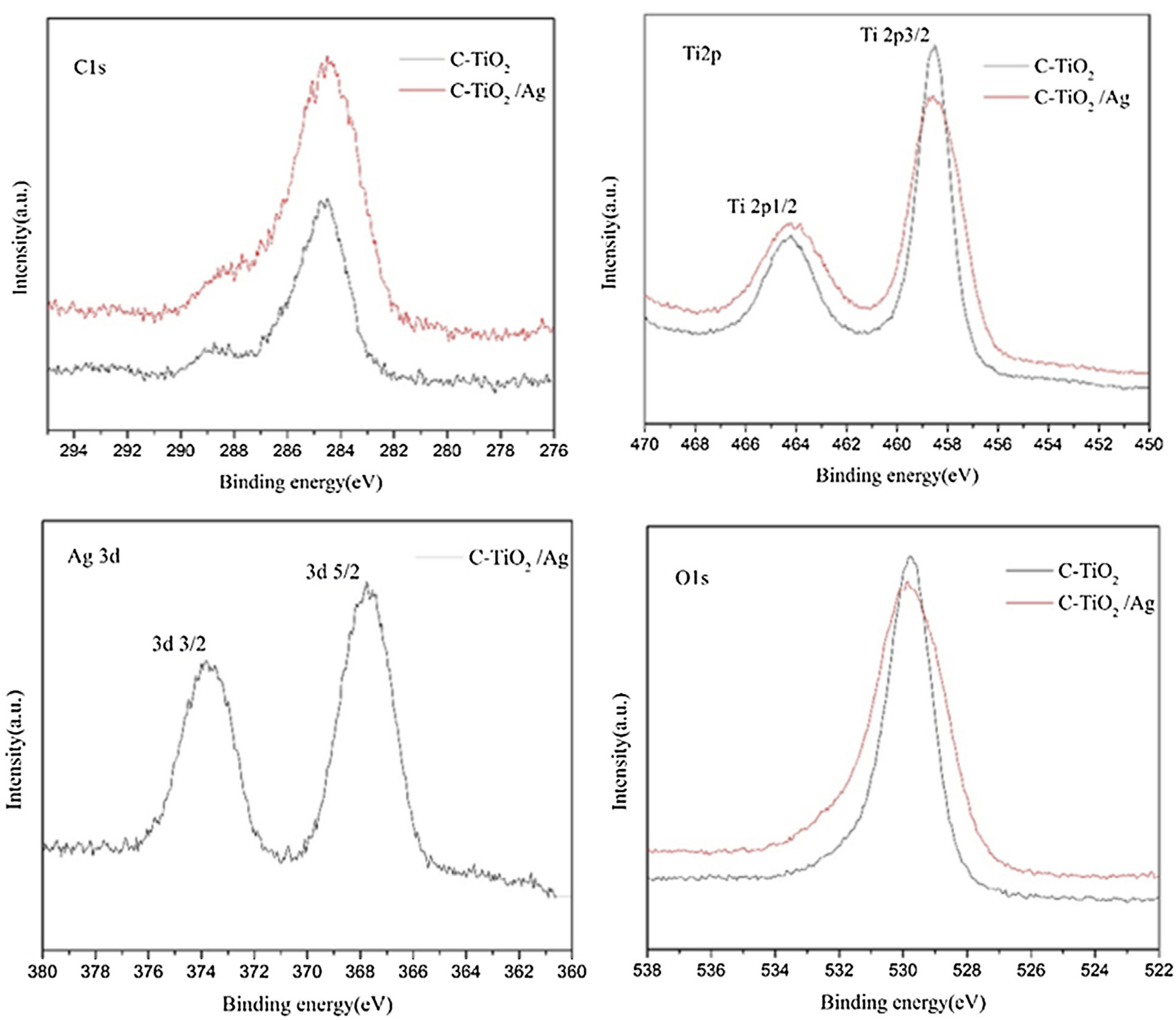

Fig. 6 XPS spectra of C1s, Ti2p, O1s, and Ag3d.

3.6. X-ray photoelectron spectroscope (XPS) indicates formation of metal Ag on C-TiO$_2$

To investigate and confirm the deposition of Ag on C-TiO$_2$ catalyst, XPS analysis was carried out and the results are shown in Fig. 6(a–d). Fig. 6(a) reflects the results of C 1s core levels. At the binding energy 284.8 eV, the C 1s peak of sample C-TiO$_2$/Ag formed a large migration than control sample (C-TiO$_2$). This result can be referred to the recent carbon species generated from heat processing. XPS peaks of Ti 2p were noticed at binding energies around 458.5 eV (Ti 2p3/2) and 464.3 eV (Ti 2p1/2), as exhibited in Fig. 6(b). The XPS of O1s was revealed one peak at binding energy 528.8 eV in the control and C-TiO$_2$/Ag as demonstrated in Fig. 6(c). On the other hand, two peaks were noticed at the 367.5 eV and 373.5 eV binding energies in C-TiO$_2$/Ag, which may be attributed to the binding energies of Ag 3d5/2 and Ag 3d3/2, respectively. These results together indicate the formation of metal Ag in the sample.

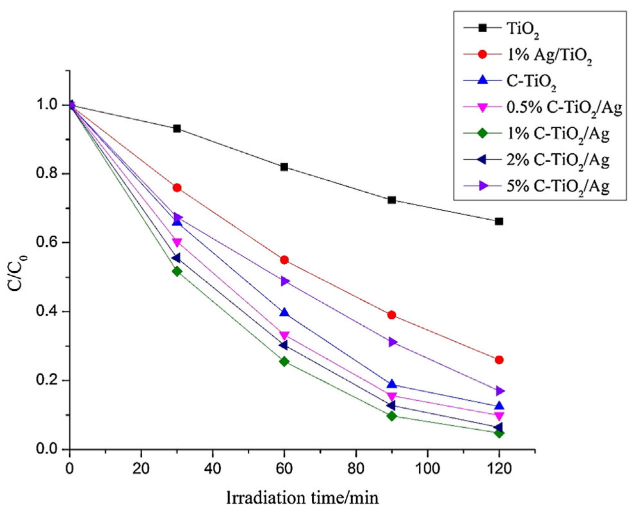

Fig. 7 Degradation of methyl orange with C-TiO$_2$ and (0.5, 1, 2, and 5 wt%Ag)/C-TiO$_2$ samples.

3.7. Silver embedding of C-TiO$_2$ (C-TiO$_2$/Ag) improves photocatalytic degradation of organic water pollutant, methyl orange

Degradation of organic pollutant, methyl orange dye under visible light irradiation was performed to test visible-light photocatalytic performance of C-TiO$_2$/Ag. The highest wavelength absorption of methyl orange in acidic form under visible light was in the range of 503 nm. Hence the difference of methyl orange absorbance was determined at 503 nm. Figs. 7 and 8 reveals the photodegradation of methyl orange by TiO$_2$, C-TiO$_2$, 1% Ag/TiO$_2$ and (0.5, 1, 2, and 5 wt%Ag) of C-TiO$_2$/Ag nanomaterials. After irradiation for 2 h, the degradation rates of methyl orange by catalysts were (33.7, 87.5, 74.4, 90.1, 95.2, 93.6, and 83.0%) for TiO$_2$, C-TiO$_2$, 1% Ag/TiO$_2$ and (0.5, 1, 2, and 5 wt%Ag) of C-TiO$_2$/Ag, respectively. High degradation rate of C-TiO$_2$ should be attributed to doping of carbon on the surface of TiO$_2$ and photosensitization of TiO$_2$. In C-TiO$_2$/Ag samples, the results showed an increased C-TiO$_2$ activity in photocatalytic degradation of methyl orange after addition of silver to C-TiO$_2$ samples.

In a previous study (Huang et al., 2018), the authors reported that optimal dispersity (0.15 g/L) of Ag particles on TiO$_2$ gave the best photocatalytic activity on Rhodamine B, while higher concentration of Ag resulted in reduced photocatalytic activity. Metal ion doping on TiO$_2$ had enhanced effect on photocatalytic activity, and doping sites could act as recombination centres for electrons and holes, thus increasing the lifetime of photogenerated electron-hole pair which increased the photoactivity (Lopez et al., 2009). Additionally, Hernandez et al. (2017) also opined that in metal doping of TiO$_2$ nanocomposites, concentration of photogenerated charge carriers and life time of electron hole recombination plays a major role in deciding photocatalytic efficiency. From the characterization results in the present study, the improvement of the degradation rate of C-TiO$_2$ after addition Ag could be attributed to the smaller crystallite size that enhances the optical absorption edge. From the results of C-TiO$_2$/Ag samples it can be concluded that the addition of Ag in ratio less than 5 wt% enhanced the photocatalytic activity of C-

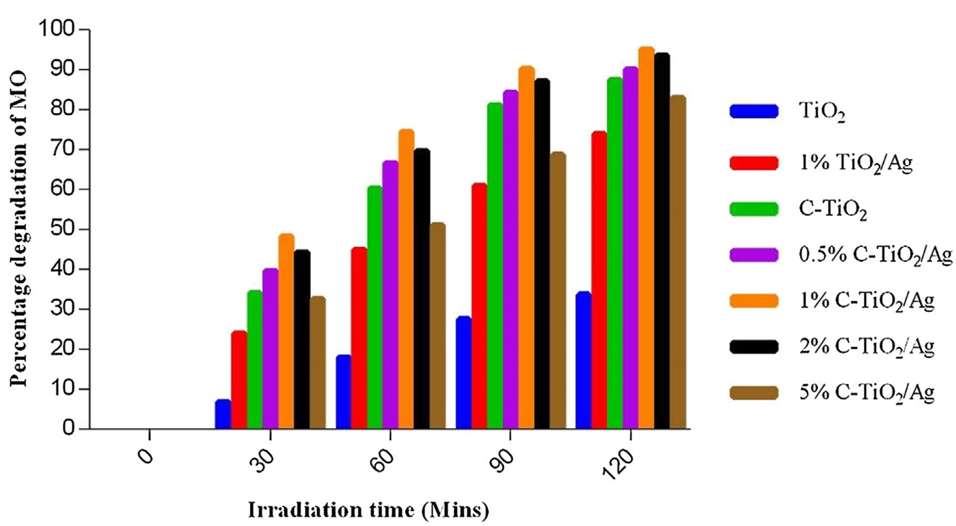

Fig. 8 Percentage degradation of methyl orange with C-TiO$_2$ and (0.5, 1, 2, and 5 wt%Ag)/C-TiO$_2$ samples.

TiO_2, and the best photodegradation rate was obtained by 1 wt % C-TiO_2/Ag.

4. Conclusions

Embedding of silver on C-TiO_2 could extend optical absorption edge of C-TiO_2 to more visible light region and inhibit electron-hole recombination resulting in enhanced photocatalytic activity. Photocatalytic degradative activity on methyl orange organic pollutant under visible light irradiation was considerably improved indicating its potential use in water treatment applications.

Acknowledgments

This research was financially supported by the National NaturalScience Foundation of China (41401547), Fok Ying-Tong Education Foundation (151078), China Postdoctoral Science Foundation (2013M540619, 2015T80855) and Open Project of State Key Labo-ratory of Freshwater Ecology and Biotechnology (2015FB04).

References

Barborini, E., Conti, A.M., Kholmanov, I., Piseri, P., Podestà, A., Milani, P., Cepek, C., Sakho, O., Macovez, R., Sancrotti, M., 2005. Nanostructured TiO2 films with 2eV optical gap. Adv. Mater. (Weinheim, Germany) 17 (15), 1842–1846.

Choi, J., Park, H., Hoffmann, M.R., 2009. Effects of single metal-ion doping on the visible-light photoreactivity of TiO2. J. Phys. Chem. C 114 (2), 783–792.

Duan, Y., Fu, N., Liu, Q., Fang, Y., Zhou, X., Zhang, J., Lin, Y., 2012. Sn-doped TiO2 photoanode for dye-sensitized solar cells. J. Phys. Chem. C 116 (16), 8888–8893.

Emeline, A., Zhang, X., Jin, M., Murakami, T., Fujishima, A., 2006. Application of a "black body" like reactor for measurements of quantum yields of photochemical reactions in heterogeneous systems. J. Phys. Chem. B 110 (14), 7409–7413.

Fang, J., Wang, F., Qian, K., Bao, H., Jiang, Z., Huang, W., 2008. Bifunctional N-doped mesoporous TiO2 photocatalysts. J. Phys. Chem. C. 112 (46), 18150–18156.

Gu, D., Lu, Y., Yang, B., 2008. Facile preparation of micro–mesoporous carbon-doped TiO2 photocatalysts with anatase crystalline walls under template-free condition. Chem. Commun. (Cambridge, United Kingdom) 21, 2453–2455.

Hernandez, J.V., Coste, S., Murillo, A.G., Romo, F.C., Kassiba, A., 2017. Effects of metal doping (Cu, Ag, Eu) on the electronic and optical behavior of nanostructured TiO2. J. Alloys Comp. 710 (5), 355–363.

Hirakawa, T., Kamat, P.V., 2005. Charge separation and catalytic activity of Ag@ TiO2 core-shell composite clusters under UV-irradiation. J. Am. Chem. Soc. 127 (11), 3928–3934.

Huang, J., Ding, L., Xi, Y., Shi, L., Su, G., Gao, R., Wang, W., Dong, B., Cao, L., 2018. Efficient silver modification of TiO2 nanotubes with enhanced photocatalytic activity. Solid State Sci. 80, 116–122.

Khan, S.U., Al-Shahry, M., Ingler, W.B., 2002. Efficient photochemical water splitting by a chemically modified n-TiO2. Science 297 (5590), 2243–2245.

Kosowska, B., Mozia, S., Morawski, A.W., Grzmil, B., Janus, M., Kałucki, K., 2005. The preparation of TiO2–nitrogen doped by calcination of TiO2xH2O under ammonia atmosphere for visible light photocatalysis. Sol. Energy Mater Sol. Cells 88 (3), 269–280.

Kumar, S.G., Devi, L.G., 2011. Review on modified TiO2 photocatalysis under UV/visible light: selected results and related mechanisms on interfacial charge carrier transfer dynamics. J. Phys. Chem. A 115 (46), 13211–13241.

Lettmann, C., Hildenbrand, K., Kisch, H., Macyk, W., Maier, W.F., 2001. Visible light photodegradation of 4-chlorophenol with a coke-containing titanium dioxide photocatalyst. Appl. Catal. B: Environ. 32 (4), 215–227.

Li, D., Haneda, H., Labhsetwar, N.K., Hishita, S., Ohashi, N., 2005. Visible-light-driven photocatalysis on fluorine-doped TiO2 powders by the creation of surface oxygen vacancies. Chem. Phys. Lett. 401 (4), 579–584.

Lopez, R., Gomez, R., Llanos, M.E., 2009. Photophysical and photocatalytic properties of nanosized copper-doped titania solegel catalysts. Catal. Today 148, 103–108.

Mai, L., Huang, C., Wang, D., Zhang, Z., Wang, Y., 2009. Effect of C doping on the structural and optical properties of sol–gel TiO2 thin films. Appl. Surf. Sci. 255 (22), 9285–9289.

Maicu, M., Hidalgo, M., Colón, G., Navío, J.A., 2011. Comparative study of the photodeposition of Pt, Au and Pd on pre-sulphated TiO2 for the photocatalytic decomposition of phenol. J. Photochem. Photobiol., A Chem. 217 (2), 275–283.

Matsubara, K., Tatsuma, T., 2007. Morphological changes and multicolor photochromism of Ag nanoparticles deposited on single-crystalline TiO2 surfaces. Adv. Mater. (Weinheim, Ger.) 19 (19), 2802–2806.

Naraginti, S., Stephen, F.B., Radhakrishnan, A., Sivakumar, A., 2015. Zirconium and silver co-doped TiO2 nanoparticles as visible light catalyst for reduction of 4-nitrophenol, degradation of methyl orange and methylene blue. Spectrochim. Acta A Mol. Biomol. Spectrosc. 25 (135), 814–819.

Ollis, D.F., Al-Ekabi, H., 1993. Photocatalytic purification and treatment of water and air: proceedings of the 1st International Conference on TiO2 Photocatalytic Purification and Treatment of Water and Air, London, Ontario, 1993 Canada, 8-13 November, 1992, Elsevier Science Ltd.

Pantelides, S.T., 1978. The electronic structure of impurities and other point defects in semiconductors. Rev. Mod. Phys. 50, 797.

Pelaez, M., Armah, A., Stathatos, E., Falaras, P., Dionysiou, D.D., 2009. Visible light-activated NF-codoped TiO2 nanoparticles for the photocatalytic degradation of microcystin-LR in water. Catal. Today 144 (1), 19–25.

Sakthivel, S., Kisch, H., 2003.. Daylight photocatalysis by carbon-modified titanium dioxide. Angew. Chem., Int. Ed. 42 (40), 4908–4911.

Subash, B., Krishnakumar, B., Swaminathan, M., Shanthi, M., 2012. Ag2S-ZnO–an efficient photocatalyst for the mineralization of Acid Black 1 with UV light. Spectrochim. Acta Part A, Mol. Biomol. Spectrosc. 105, 314–319.

Tom, R.T., Nair, A.S., Singh, N., Aslam, M., Nagendra, C., Philip, R., Vijayamohanan, K., Pradeep, T., 2003. Freely dispersible Au@ TiO2, Au@ ZrO2, Ag@ TiO2, and Ag@ ZrO2 core-shell nanoparticles: one-step synthesis, characterization, spectroscopy, and optical limiting properties. Langmuir 19 (8), 3439–3445.

Ung, T., Liz-Marzán, L.M., Mulvaney, P., 1998. Controlled method for silica coating of silver colloids. Influence of coating on the rate of chemical reactions. Langmuir 14 (14), 3740–3748.

Xu, L., Steinmiller, E.M., Skrabalak, S.E., 2011. Achieving synergy with a potential photocatalytic Z-scheme: synthesis and evaluation of nitrogen-doped TiO2/SnO2 composites. J. Phys. Chem. C 116 (1), 871–877.